厚生労働省科学研究費補助金（新興・再興感染症研究事業）
分担研究報告書

桂皮および丁子エキスによるSARS-Covの侵入阻止効果

分担研究者：服部 俊夫　東北大学大学院医学系研究科教授

研究要旨：桂皮樹皮エキス(CCE)と丁子エキス(CFE)の抗SARS能の詳細な検討を行った。SARSコロナウイルスとVSVはエンドサイトーシス経路を経て細胞内に侵入する。ウイルスのとるエンドサイトーシス経路は、クラスリン依存とクラスリン非依存性の経路がある。VSVはトランスフェリン受容体(Tfr)と同じくクラスリン依存性である。CD59はクラスリン非依存性でエンドサイトーシス経路をとる。TfrとCD59のリサイクリングは、細胞表面上で検出可能であるので、われわれは薬草がこれらの分子の発現に影響するかどうかをJurkat細胞についてフローサイトメトリーによって検証した。

■研究協力者
庄敏　（財団法人ヒューマンサイエンス振興財団）
秦川　（中国協和医科大学　実験動物研究所）
大島吉輝（東北大学大学院薬学研究科）

A. 研究目的

SARSウイルスの感染には、自身のスパイク蛋白質と標的細胞膜上のアンギオテンシン転換酵素2型(ACE2)との結合が必要である。われわれはこれまでに、上記の過程を解析するために、HIV/SARS-CoV S偽ウイルスとHIV/VSVG偽ウイルスを作成し、偽ウイルス感染系を確立した。さらに、293T細胞にSARSウイルスS蛋白質を発現させ、これとHela-ACE2との融合を検出する細胞膜融合系も確立した。これらの系を用いて、SARSウイルスの感染を抑制する物質のスクリーニングを行い、漢方薬として用いられている丁子と桂皮のエキスに感染抑制効果のあることを明らかにした。これらのエキスは、SARSウイルス野生株を用いた感染実験においても効果を示した。

今年度は、エキスの効果を詳細に検討するために、SARSウイルスのエンドサイトーシスがエキスによってどのような影響を受けるのか、細胞表面上に発現している分子のリサイクリングを中心に観察することとした。

B.材料と方法

細胞株

293T, HepG2, VeroE6, Jurkat 細胞は東北大学加齢医学研究所医用細胞資源センターから提供を受けた。

漢方薬エキスの抽出・精製・同定

17 種類の化合物を HIV/SARS-CoV S 偽ウイルス感染抑制実験に用いた（文末付表参照)。

ベクターと偽ウイルスの作成

HIV/SARS-CoV S および HIV/VSVG 偽ウイルスを作成するために pCMVΔR8.2 と pHR'CMV-Luc に pCMV/R-SARS–S または pMD.G を 293T 細胞に共導入した。偽ウイルスの定量は、p24 enzyme-linked immunosorbent assay (ZeptoMetrix Corporation, New York)で行った。

偽ウイルス系を用いた感染抑制

HepG2 (1×10^4 cells/well)を 96-well に感染前日に播種した。5 ng (p24) の HIV/SARS-CoV S または HIV/VSVG 偽ウイルスを加え 37°C、30 分間培養した。実験群には、ウイルスと一緒に植物エキスを加えた。感染後 12 時間たって細胞を DMEM で二度洗浄し培地を交換した。48 時間後、ルシフェラーゼ活性を Mithras LB940 (Berthold Technologies GmbH&Co KG, Germany)で測定した。相対的なルシフェラーゼ活性を測定し、50%抑制濃度(IC50)を求めた。

SARS-CoV 野生株感染実験

SARS-CoV 野生株の一つである PUMC01 F5 (GenBank AY350750)を用いた。VeroE6 細胞を用いて感染 3 又は 4 日後の $TCID_{50}$ によって 1ml あたりのウイルス量を決定した。10 $TCID_{50}$ の SARS-CoV 野生株を 100μl 用い 37℃ で 30 分間培養した。前日に VeroE6 細胞を播種した 96-well plates (4×10^4 cells/well) にこれを加えた。1 時間静置した後、DMEM で細胞洗浄を行い培地交換を行った。72 時間培養の後、細胞変性効果(CPE)を測定した。ウイルス複製の 50%抑制濃度は、CPE 観察を行い Reed-Muench 法によった。

プラークリダクションアッセイでは、100 $TCID_{50}$ の SARS-CoV 野生株 100 μl、漢方薬エキスと共に 37℃30 分間処理した後、Vero E6 細胞と共に 6 well plates (1×10^6 cells/well) で培養した。 1 時間培養の後、細胞を DMEM で洗浄し、2%アガロースを加え、0.05%ニューラルレッドを加えた 2%二次アガロースを培養 3 日目に追加した。24 時間で生ずるプラークの数を数え、IC_{50} を求めた。

細胞毒性分析

細胞毒性の検討は、偽ウイルス感染実験と同じ条件で行った。HepG2細胞1×10^4個を96ウェルplateで培養し、24時間後に漢方薬エキスを加えた。14時間培養の後、細胞洗浄を行い、DMEMを加えた。CCK-8試薬を加えた後に4時間後OD450を読み取り50%成長抑制の濃度を決定した。

フローサイトメトリー分析

Jurkut細胞に漢方薬エキスを加え、濃度と培養時間を変化させて感染抑制効果を検討した。細胞は、PBS (0.1% BSA) で2回洗浄した。 anti-CD59-FITC (BD Biosciences)と anti-Tfr-PE (BD Biosciences)を加え30分間4°Cで培養した後、フローサイトメーター (Beckman Coulter, Fullerton, CA, USA)にかけて、CXP Analysis software version 2.0で分析を行った。

蛍光Transferrin-A488の取り込み

JurkutT細胞は、PBSで2回洗浄し0.1mg/mlのCCEまたはCCEの第二画分を加えon ice

で30分間培養した。A488でラベルしたtransferrin (Molecular Probes)を10^7 cells/mlについて50 mg/ml相当の濃度になるように加え、30分間培養した。蛍光励起の後PBSで2回洗浄しエキスの最終濃度が0.1mg/mlとなるように調整、37℃で15分間培養した。培養時間の経過後サインプルをon iceに移しPBSで冷却して反応を停止させた。細胞を4% paraformaldehydeで固定しpolyl-lysine処理したカバーガラス(Sigma-Aldrich)に塗布しZeiss LSM510で蛍光観察を行った。

C.結果

偽ウイルス感染の抑制

スクリーニングを行った7種類の漢方薬のうち、CCEとCFEのみが100μg/mlという低いIC50を示し、その抑制活性は濃度依存性であった。CCEとCFEの両方がHIV/VSVGの感染を抑制した。

CCについてエタノール抽出を行い、4つの画分の感染抑制効果を検討した。水層(Fr.3)とAcOEt層(Fr.4)は活性を示さなかったため、aq.EtOH層(Fr.1)とCC-Bu(Fig.2A, B)の結果のみを示す。偽ウイルスは、感染した細胞の中で一度だけ複製するが、ルシフェラーゼ活性は、侵入過程のみを検出するわけではない。そのために、CCE、CFE、CC-Buの抑制効果の時間依存性を検討した。HIV/SARS-CoV S 偽ウイルスをチャレンジする1時間前と10時間後にエキスを加え、感染抑制効果を検討した。ウイルスチャレンジの前にエキスを追加した条件でのみ感染抑制効果がみられた。ことのことは、エキスはHIV/SARS-CoV S感染初期の過程を抑制する効果を持つことを示す。
のみを示す。偽ウイルスは、感染した細胞の中で一度だけ複製するが、ルシフェラーゼ活性は、侵入過程のみを検出するわけではない。そのために、CCE、CFE、CC-Buの抑制効果の時間依存性を検討した。HIV/SARS-CoV S 偽ウイルスをチャレンジする1時間前と10時間後にエキスを加え、感染抑制効果を検討した。ウイルスチャレンジの前にエキスを追加した条件でのみ感染抑制効果がみられた。ことのことは、エキスはHIV/SARS-CoV S感染初期の過程を抑制する効果を持つことを示す。

SARS-CoV 野生株への感染抑制効果

プラークリダクションアッセイによって感染抑制効果を定量的に検討した。CCE と CFE の両方、感染の前に細胞を処理した条件でSARS-CoV の感染を抑制した(Table.1)。偽ウイルス感染実験と同様に、ウイルスをチャレンジしたあとにエキスを投与しても感染抑制効果はみられなかった。このことからエキスは感染の初期の段階に作用することが示唆される。CCの4つの画分のうち、ブタノール画分はプラークリダクションアッセイで高い抑制活性を示し、SI は CCE、CC のブタノール画分と比べても高く、より活性の高い物質が含まれている。

Jurkut 細胞膜上の CD59、Tfr 発現に対する漢方薬の影響

CCE と CFE は SARS-CoV 感染を抑制するばかりでなく、HIV/VSVG の感染も抑制する。そこで、漢方薬エキスがエンドサイトーシス経路に影響している可能性を検討した。Tfr はクラスリン依存性のエンドサイトーシスの指標となり CD59 はクラスリン非依存性のエンドサイトーシスの指標として利用可能である。予想に反して、CC-Bu

と CCE は Tfr の発現を抑制し、それは時間・濃度依存的であった(図 1A)。これに対して、CD59 の発現はエキスの影響を受けなかった(図 1B)。さらに、CC の第 3 画分も CFE も Tfr や CD59 の発現に影響しなかった。これらの結果は、CC の抗ウイルス効果は Tfr のエンドサイトーシス経路に影響することを示唆する。

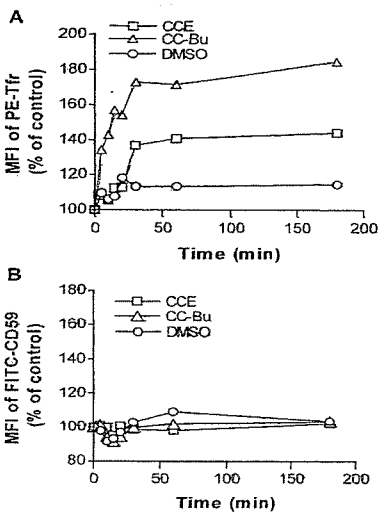

図1:桂皮エキス（CCE）のSARSウイルス感染抑制効果
A.CC-BuとCCEは時間・濃度依存的にTfrの発現を抑制する。B.これらは、CD59の発現には影響しない。

蛍光 Transferrin-A488 の取り込み

Jurkut細胞膜上のTfn-A488はCCEやCCEの第 2 画分のない条件で取り込まれた。これらの成分は 0.1mg/ml で Tfr の取り込みを抑制した（図 2)。

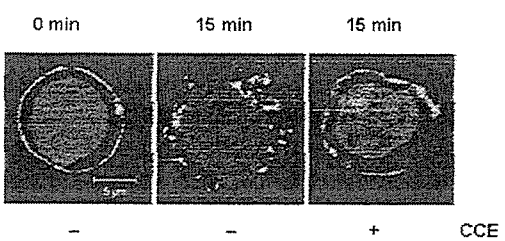

図 2:Tm-A488 の取り込み
核を DAPI 染色した。エキス非存在下では、Tfn-A488 は細胞質に分布するが（中)、0.1 mg/ml の CCE が存在すると細胞表面に分布する（右)。

D.考察

CCEとCFEはSARS-CoVの感染初期過程を抑制することが、偽ウイルスと野生株を用いた感染実験によって明らかになった。風邪薬として用いられているCCも、活性成分の同定にまでは至らなかったが、SARS-CoV の感染を抑制した。CCの抗ウイルス活性を明らかにするため、精製画分の感染抑制効果を偽ウイルスを用いて検証し、ブタノール画分に最も強力な抑制活性があることを示した。プラークリダクションアッセイではCCのブタノール画分のIC_{50}は他のエキスの抑制活性と比較して強力であったことから、CCの有効成分はこの画分に存在していることが示唆された。CCの抗ウイルス活性成分はエピカテキンとタンニン酸であるとされるが、これらはHIV/SARS-CoV S偽ウイルスの感染抑制効果を示さなかった。CCの抗SARSウイルス活性成分の探索にはさらなる研究が必要である。

CCE と CFE は SARS-CoV だけでなく HIV/VSVG 偽ウイルスの感染も抑制したことから、これらのエキスは両方のウイルスに共通する経路を阻害している可能性を検討した。VSV や多くのエンベロープ・ウイルスの感染が成立するには、細胞内に取り込まれ初期エンドソーム、後期エンドソーム、リソソームという経路を利用する必要がある。VSV の感染は PH 依存であることが知られている。最近 VSV はクラスリン依存性のエンドサイトーシス経路を利用することが明らかになった。SARS-CoV も PH 依存的に細胞内に侵入する。しかし、エンドサイトーシスの経路は明らかになっていない。CD59 と Tfr はリサイクルをする代表的なクラスリン依存性のエンドサイトーシ

スの指標物質であることから、CCE と CFE がこれらの物質のリサイクリング経路を阻害するかどうかを検討した。予想に反して、CC-Bu と CCE は Tfr の発現を上昇させ、それは時間・濃度依存的であった [Fig.3]。Tfr はクラスリン依存性にリサイクルをする分子であり、リサイクルが阻害されると細胞表面上の発現が上昇すると考えられる。これらのことから、CC-Bu にはクラスリン系の経路を阻害する因子が含まれていると考えられる。しかしながら、CC-Bu には様々な成分が含まれており、活性を示す因子は単独の成分であるのか、複数の成分によるものなのかは現時点では明らかではない。CD59 の発現が増強されないということから、これらの因子は非クラスリン系の経路には影響しないかもしれないということに注目すべきである。VSV の感染において Epsin15 がクラスリン系の経路に必須の蛋白質であることと、トランスフェリンのリサイクリングに関与していることが指摘されている。しかし、われわれの実験結果からは、感染抑制を示したエキスに含まれているどの分子が作用するのかは特定できなかった。CC-Bu 画分の詳細な検討を行って、ウイルス侵入と受容体のリサイクリングというウイルス感染に共通する機序の解明を試みたい。

E.結論

桂皮エキスと丁子エキスが、SARS ウイルスの感染を抑制することをスクリーニングによって明らかにした。ウイルスがどのような経路で細胞に取り込まれるのか、その過程を解析し、エキスの効果の詳細な検討を行った。その結果、それらのうち桂皮のブタノール画分に強力な感染抑制因子が含まれていることが明らかになった。

F.健康危険情報

該当事項無し

G研究発表

論文

1.Osamu Usami, Yugo Ashino, Yuichi Komaki, Masafumi Tomaki, Toshiya Irokawa, Tsutomu Tamada, Tsunefusa Hayashida, Katsuji Teruya and Toshio Hattori. Efavirenz induced neurological symptoms in rare homozygote CYP2B6 *2/*2 (C64T). International Journal of STD & AIDS, accepted

2.Tamada T, Nara M, Tomaki M, Ashino Y, Hattori T. Secondary bronchiolitis obliterans organising pneumonia in a patient with carbamazepine-induced hypogammaglobulinemia. Thorax. 2007 Jan;62(1):100.

3.Usami, O., Xiao, P., Hong Ling, H. and Hattori, T. Competitive Study of Monoclonal Antibodies Against the HIV-1 Gp41 Core Structure Microbiology and Immunology 50: 131-134, 2006

4.Di Li, Hong-Xi Gu, Shu-Yun Zhang, Zhao-Hua Zhong, Min Zhuang, Toshio HattoriYMDD mutations and genotypes of HBV in Northern China J J Infectious Diseases 59:42-45, 2006

5.Guio, H.; Okayama, H.; Ashino, Y.; Saitoh, H.; Xiao, P.; Miki, M., Yoshihara, N., Nakanowatari, S., Hattori, T. Method for efficient storing and transport of

sputum specimens for molecular testing of tuberculosis. The Int. J. Tb Lung Dis. 10:906-10. 2006

6.Nara M, Sano K, Ogawa H, Tamada T, Nagaoka M, Okada K, Watanabe M, Moriya T, Miki H, Nakata K, Ichinose M, Hattori T. Serum Antibody Against Granulocyte/Macrophage

7.Colony-Stimulating Factor and KL-6 in Idiopathic Pulmonary Alveolar Proteinosis. Tohoku J Exp Med. 2006 Apr;208(4):349-54.

8.Tomaki M, Sugiura H, Koarai A, Komaki Y, Akita T, Matsumoto T, Nakanishi A, Ogawa H, Hattori T, Ichinose M. Decreased expression of antioxidant enzymes and increased expression of chemokines in COPD lung. Pulm Pharmacol in press

学会発表

1. Xiao, P., Ling, H., Usami, O., Furuta, R. A., Shimizu, N., Hoshino, H., Zhuang, M., Hattori, T. Characterization of a CD4-independent primary HIV-1 isolate from Pneumocystis Pneumonia patient. 10th Anniversary Annual International Meeting of the Institute of Human Virology, Novermber 17-19, 2006, Hyatt Regency Baltimore, Baltimore, Maryland, U.S.A.

2. 庄敏, 蒋虹, 古田理佳, 肖鵬, 服部俊夫.The inhibitory effect of medical herbs on SARS-CoV entry in vitro. 第５４回日本ウイルス学会学術集会, 11 月 19 日-21 日, 2006, 名古屋国際会議場 イベントホール

付表：抗 SARS ウイルス活性のスクリーニングに用いた化合物

Num	Compounds	MW	Molecular formular	Formula	IC50	CC50	SI
C1	trans-Cinnamaidenyde	132.16	$C_6H_5CH=CHCHO$	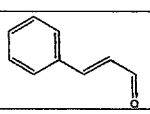	0.003%	0.002-0.003%	1
C2	(-)-Epicatechin	290.27	$C_{15}H_{14}O_6$	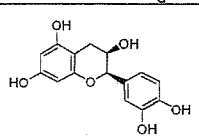	2 mg/ml	1-3mg/ml	1
C3	Trans-cinnamic acid	148.16	$C_9H_8O_2$	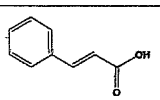	3 mM	22.55 mM	7.5
C4	Licochalcone-A synthetic	338.4			0.03-0.1 mM	0.025 mM	1-2
C5	2-phenylethanol (phenethy alcohol)	122.17	C6H5(CH2)2OH	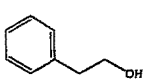	0.05%	0.3%	6
C6	2'-hydroxyacetophenone (o-hydroxyacetophenone)	136.15	C8H8O2	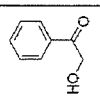	0.25%	0.25%	1

C7	isoeugenol	164.20	C10H12O2	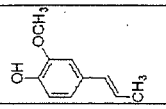	>0.03125 %	0.0625%	<2
C8	2-hydroxycinnamic acid	164.16	HOC6H4CH=COOH	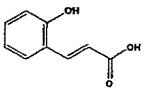	0.3 mM	2.5-5 mM	>8.3
C9	3,4-dimethoxycinnamic acid	208.21	C11H12O4	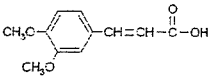	>5mM	>10 mM	>2
C10	4-hydroxy-3-methoxycinnamic acid (ferulic acid)	194.18	C10H10O4	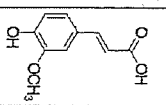	5mM	>10 mM	>2
C11	4-hydroxy-3-methoxy cinnamaldehyde	178.18	HOC6H3(OCH3)CH =CHCHO	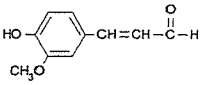	0.34-0.67 mM	0.67-1.06 9 mM	1-2
C12	4-hydroxycoumarin	162.14	C9H6O3	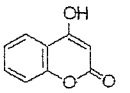	>10mM	>10mM	1
C13	7-hydroxycoumarin	162.14	C9H6O3		>2.5mM	>10mM	4
C14	p-cymene	134.22	CH3C6H4CH(CH3)2	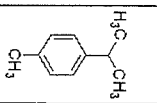	>1%	1%	<1
C15	4-allylanisole	148.20	$H_2C=CHCH_2C_6H_4OCH_3$	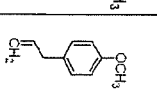	>0.125%	>0.25%	<1
C16	ethylcinnamate	176.21	C6H5CH=CHCOOC H2CH3	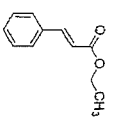	>0.125%	>0.25%	<1
C17	cinnamylacetate	176.21	C11H12O2	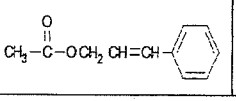	>0.125%	0.25%	<1

III. 研究成果の刊行に関する一覧表

研究成果の刊行に関する一覧表レイアウト

雑誌

発表者氏名	論文タイトル名	発表誌名	巻号	ページ	出版年
Kyuuma, M, Kikuchi, K, Kojima, K, Sugawara, Y, Sato, M, Mano, N, Goto, J, Takeshita, T, Yamamoto, A, **Sugamura, K** and Tanaka, N.	AMSH, an ESCRT-III Associated Enzyme, Deubiquitinates Cargo on MVB/Late Endosomes.	Cell Struct Funct	31	159-172	2006
Chen, S., Ishii, N., Ine, S., Ikeda, S., Fujimura, T., Ndhlovu, L. C., Soroosh, P., Tada, K., Harigae, H., Kameoka, J., Kasai, N., Sasaki, T. and **Sugamura, K**	Regulatory T cell-like activity of Foxp3^{+} adult T cell leukemia cells	*Int. Immunol.*	18	269-277	2006
Ishikawa, Y., Tanaka, N., Murakami, K., Uchiyama, T., Kumaki, S., Tsuchiya, S., Kugoh, H., Oshimura, M., Calos, M. P. and **Sugamura, K**	Phage fC31 integrase-mediated genomic integration of the common cytokine receptor gamma chain in human T-cell lines	*J. Gene Medicine*	8	646-53	2006
Satoh, K., Kagaya, Y., Nakano, M., Ito, Y., Ohta, J., Tada, H., Karibe, A., Minegishi, N., Suzuki, N., Yamamoto, M., Ono, M., Watanabe, J., Shirato, K., Ishii, N., **Sugamura, K.** and Shimokawa, H	Important role of endogenouserythropoietin system to recruit endothelial progenitor cells in hypoxia-induced pulmonary hypertension in mice	*Circulation*	113	1442-1450	2006
Soroosh, P., Ine, S., **Sugamura, K.** and Ishii, N	OX40-OX40 ligand interaction through T cell-T cell contact contributes to CD4 T cell longevity	*J. Immunol*	176	5975-5987	2006

Uchiyama, T., Kumaki, S., Ishikawa, T., Onodera, M., Sato, M., Du, W., Sasahara, Y., Tanaka, N., **Sugamura, K.** and Tsuchiya, S	Application of HSVtk suicide gene to X-SCID gene therapy: Ganciclovir offsets gene corrected X-SCID B cells. *Biochem*	*Biophy. Res. Comm.*	341	391-8	2006
Nakashima, A., Tanaka, N., Tamai, K., Kyuuma, M., Ishikawa, Y., Sato, H., Yoshimori, T., Saito, S. and **Sugamura, K**	Survival of parvovirus B19 infected cells by cellular autophagy	*Virology*	349	254-263	2006
Watanabe, R., Harada, Y., Takeda, K., Takahashi, J., Ohnuki, K., Ogawa, S., Kaibara, N., Koiwai, O., Tanabe, K., Toma, H., **Sugamura, K.** and Abe, R	Grb2 and Gads exhibit different interactions with CD28 and play distinct roles in CD28-mediated costimulation	*J. Immunol*	177	1085-1091	2006
Satoh, T., Moroi, R., Aritake, K., Urabe, Y., Kanai, Y., Sumi, K., Yokozeki, H., Hirai, H., Nagata, K., Hara, T., Utsumi, M., Hirokawa, K., **Sugamura, K.**, Nishioka, K., Nakamura, M	Prostablandin D2 plays an essential role in chronic allergic inflammation of the skin via CRTH2 receptor	*J. Immunol.*, in press			

研究成果の刊行に関する一覧表レイアウト

雑誌

発表者氏名	論文タイトル名	発表誌名	巻号	ページ	出版年
Hoshino S, Sun B, Konishi M, Shimura M. Segawa T, Hagiwara Y, Koyanagi Y, Iwamoto A, Mimaya J, Terunuma H, Kano S and **Ishizaka Y**	Vpr in plasma of HIV-1-positive patients is correlated with the HIV-1 RNA titers	*AIDS Res. Hum. Retrovir.* In press.			
Nakai-Murakami C, Shimura M, Kinomoto K, Takizawa Y, Tokunaga K, Taguchi T, Hoshino S, Miyagawa K, Sata T, Kurumizaka H, Yuo A and **Ishizaka Y**	HIV-1 Vpr induces ATM-dependent cellular signal with enhanced homologous recombination	*Oncogene*	26	477-486	2007
Tachiwana H, Shimura M, Nakai-Murakami C, Tokunaga K, Takizawa Y, Sata T, Kurumizaka H, **Ishizaka Y**	HIV-1 Vpr induces DNA double-strand breaks	Cancer Res	66	627-631	2006

研究成果の刊行に関する一覧表レイアウト

雑誌

発表者氏名	論文タイトル名	発表誌名	巻号	ページ	出版年
Zhang J and **Hattori T**	Small RNA molecules as therapeutic genes for viral infectious diseases.	In Journal of Pharmacology and Toxicology			in press
Osamu Usami, Yugo Ashino, Yuichi Komaki, Masafumi Tomaki, Toshiya Irokawa, Tsutomu Tamada, Tsunefusa Hayashida, Katsuji Teruya and Toshio Hattori.	Efavirenz induced neurological symptoms in rare homozygote CYP2B6 *2/*2 (C64T).	International Journal of STD & AIDS			accepted
服部俊夫、巽浩一郎、岩垣博己、佐久間光江	**ウイルス感染とバイオディフェンス**	Mebio 別冊	24	16-21	2007
Tamada T, Nara M, Tomaki M, Ashino Y, Hattori T.	Secondary bronchiolitis obliterans organising pneumonia in a patient with carbamazepine-induced hypogammaglobulinemia.	Throax	Jan;62(1)	100	2007
Nara M, Sano K, Ogawa H, Tamada T, Nagaoka M, Okada K, Watanabe M, Moriya T, Miki H, Nakata K, Ichinose M, **Hattori T**	Serum Antibody Against Granulocyte/Macrophage Colony-Stimulating Factor andKL-6 in Idiopathic Pulmonary Alveolar Proteinosis	Tohoku J Exp Med	208(4)	349-54	2006
Usami, O., Xiao, P., Hong Ling, H. **Hattori, T**	Competitive Study of Monoclonal Antibodies Against the HIV-1 Gp41 Core Structure	Microbiology and Immunology	50	131-134	2006
Di Li, Hong-Xi Gu, Shu-Yun Zhang, Zhao-Hua Zhong, Min Zhuang, **Toshio Hattori**	YMDD mutations and genotypes of HBV in Northern China	J J Infectious Diseases	59	42-45	2006

Guio, H. Okayama, H. Ashino, Y. Saitoh, H. Xiao, P. Miki, M. Yoshijara, N. Nakanowatari, S. Hattori, T	Method for efficient storing and transport of sputum specimens for molecular testing of tuberculosis	The Int J Tb Lung Dis	10 (8)	906-10	2006
服部俊夫、芦野有悟、宇佐美修、古田里佳	HIVの感染と増殖のメカニズム	診断と治療	94	2208-2212	2006

IV. 研究成果の刊行物・別刷

CELL STRUCTURE AND FUNCTION 31: 159–172 (2006)

AMSH, an ESCRT-III Associated Enzyme, Deubiquitinates Cargo on MVB/Late Endosomes

Masanao Kyuuma[1,6], Kazu Kikuchi[1,6], Katsuhiko Kojima[2], Yuriko Sugawara[1], Mariko Sato[1], Nariyasu Mano[3], Junichi Goto[3], Toshikazu Takeshita[2], Akitsugu Yamamoto[4], Kazuo Sugamura[1], and Nobuyuki Tanaka[1,5]*

[1]Department of Microbiology and Immunology, Tohoku University Graduate School of Medicine, 2-1 Seiryo-machi, Sendai, 980-8575, Japan, [2]Department of Microbiology and Immunology, Shinshu University School of Medicine, 3-1 Asahi, Matsumoto, 390-8621 Japan, [3]Tohoku University Graduate School of Pharmaceutical Sciences, Aobayama, Sendai, 980-8578, Japan, [4]Faculty of Bioscience, Nagahama Institute of Bio-Science and Technology, Nagahama, Shiga, 526-0829, Japan, [5]Division of Immunology, Miyagi Cancer Center Research Institute, Miyagi, 981-1293 Japan, and [6]These two authors contributed equally to this work.

ABSTRACT. **The appropriate sorting of vesicular cargo, including cell-surface proteins, is critical for many cellular functions. Ubiquitinated cargo is targeted to endosomes and digested by lysosomal enzymes. We previously identified AMSH, a deubiquitination enzyme (DUB), to be involved in vesicular transport. Here, we purified an AMSH-binding protein, CHMP3, which is an ESCRT-III subunit. ESCRT-III functions on maturing endosomes, indicating AMSH might also play a role in MVB/late endosomes. Expression of an AMSH mutant lacking CHMP3-binding ability resulted in aberrant endosomes with accumulations of ubiquitinated cargo. Nevertheless, CHMP3-binding capability was not essential for AMSH's *in vitro* DUB activity or its endosomal localization, suggesting that, *in vivo*, the deubiquitination of endosomal cargo is CHMP3-dependent. Ubiquitinated cargo also accumulated on endosomes when catalytically inactive AMSH was expressed or AMSH was depleted. These results suggest that both the DUB activity of AMSH and its CHMP3-binding ability are required to clear ubiquitinated cargo from endosomes.**

Key words: deubiquitination/endosome/ESCRT-III/MVB/ubiquitin

Introduction

The endosomal system of mammalian cells forms a dynamic membranous network by which membrane proteins are transported and/or degraded. A variety of cell-surface proteins are endocytosed and translocated to early endosomes as cargo. Although some receptors are recycled back to the cell surface, cargo destined to be degraded is sorted into the multivesicular body (MVB) (Hicke, 2001; Katzmann *et al.*, 2002). Cargo proteins concentrated on the limiting membranes of the MVB are internalized by invagination, and the membrane is pinched off to form intraluminal vesicles (Gruenberg and Stenmark, 2004). Thus, MVB sorting of proteins exposes them to degradation by lysosomal enzymes.

Accumulating evidence suggests that cargo sorting and MVB formation require at least 18 conserved molecules, called the class E Vps proteins (Babst, 2005). Mutation of any of the genes encoding these proteins in yeast results in the formation of an aberrant endosome called the "class E compartment." Class E Vps proteins are highly conserved between yeast and mammals, and their mutation or deletion in mammals results in the formation of a similar class E structure (Kanazawa *et al.*, 2003; Kobayashi *et al.*, 2005). These Vps proteins are constituents of at least four separate heteromeric protein complexes called ESCRT-0 (Endosomal Sorting Complex Required for Transport-0, also known as the STAM-HRS complex), ESCRT-I, ESCRT-II,

*To whom correspondence should be addressed: Nobuyuki Tanaka, Department of Microbiology and Immunology, Tohoku University Graduate School of Medicine, 2-1 Seiryo-machi, Sendai, 980-8575 Japan.
Tel: +81–22–717–8096, Fax: +81–22–717–8097
E-mail: n-tanaka@mail.tains.tohoku.ac.jp

Abbreviations: AMSH, associated molecule with the SH3 domain of STAM; AMSH-LP, AMSH-like protein; DUB, deubiquitinating enzyme; STAM1 and STAM2, signal transducing adaptor molecule 1 and 2; Hrs, hepatocyte growth factor-regulated tyrosine kinase substrate; MVB, multivesicular bodies; ESCRT, endosomal sorting complexes required for transport; EGF, epidermal growth factor; Vps, vacuolar protein sorting; shRNA, short hairpin RNA.

and ESCRT-III.

Cargo first captured by ESCRT-0 on early endosomes is handed off to ESCRT-I and subsequently to ESCRT-II. Close to the final step of sorting, the ESCRT-III complex, which is composed of CHMP1, CHMP2, CHMP3, CHMP4, CHMP5, and CHMP6, concentrates the cargos on the maturing endosomes (Raiborg *et al.*, 2003; Gruenberg and Stenmark, 2004; Morita and Sundquist, 2004). Finally, additional class E VPS proteins, Vps4A and Vps4B, dissociate the ESCRT complex from the endosomal membrane in an ATP-dependent manner, allowing the cargo to be invaginated into the MVB (Babst *et al.*, 1997).

The MVB sorting machinery is mediated by ubiquitination. Ubiquitin is a highly conserved protein of 76 amino acids that can be covalently conjugated to specific protein substrates by a cascade of ubiquitin-conjugating enzymes, including catalytic proteins called E3. Ubiquitination was first identified as polyubiquitin chains on target proteins, which lead the proteins to be degraded by proteasomes (Weissman, 2001; Glickman and Ciechanover, 2002). In contrast, monoubiquitination of proteins was shown to target the proteins to the MVB pathway (Bonifacino and Traub, 2003). The single ubiquitin moiety is recognized by a variety of proteins involved in cargo sorting, through their various ubiquitin-interacting domains. In the initial sorting events after monoubiquitination, the ubiquitin moiety is first recognized by the UIM and VHS domains of STAM and Hrs (Asao *et al.*, 1997; Mizuno *et al.*, 2003). Likewise, the UEV domain of the ESCRT-I subunit Tsg101 also functions in cargo sorting (Katzmann *et al.*, 2002). Thus, ubiquitination is very important for the accurate sorting of cargo.

In studies aimed at finding molecules associated with STAM, we identified the AMSH deubiquitinating (DUB) enzyme (Tanaka *et al.*, 1999; McCullough *et al.*, 2004). AMSH possesses an isopeptidase domain characterized by the JAB1/MPN/Mov34 metalloenzyme (JAMM) domain. In an *in vitro* assay, recombinant AMSH removed ubiquitin moieties from K63-linked but not K48-linked ubiquitins (McCullough *et al.*, 2004). Since K63 ubiquitin, like monoubiquitin, is associated with cargo sorting, the K63-specific DUB activity suggested that AMSH might function in MVB cargo sorting. However, a genetic approach in yeast failed to identify any AMSH orthologues in MVB sorting. Indeed, there is no evidence from the database that yeast possesses an AMSH orthologue. Instead, yeast has a DUB called Doa4 that functions in MVB sorting proximal to the last steps (Swaminathan *et al.*, 1999; Amerik *et al.*, 2000; Katzmann *et al.*, 2001; Babst *et al.*, 2002; Luhtala and Odorizzi, 2004). Thus, it has been unclear whether a DUB is involved in MVB sorting in mammals.

To further characterize the function of AMSH in MVB formation and/or protein sorting, we sought AMSH-binding proteins. Here we provide evidence that AMSH is involved in cargo sorting on MVB/late endosomes through its binding to the ESCRT-III complex.

Materials and Methods

Cell culture

HeLa and 293T cells were cultured in Dulbecco's modified Eagle's medium (DMEM) supplemented with 10% fetal calf serum (FCS) and antibiotics, under 7% CO_2 in a humidified incubator. FuGENE™6 transfection reagent (Roche) was used to transfect the cells with plasmid DNAs, following the manufacturer's protocol. For cross-linking experiments, cells were suspended in 10 ml PBS containing 1 mM $MgSO_4$ (pH 8.3) and 100 μg/ml DSP (Pierce) on ice for 20 min, then washed extensively with PBS. Cell lysates were prepared and used for further experiments, as described below. For EGF stimulation experiments, cells were incubated with 200 μM E-64-d and 20 μM pepstatin A (Peptide Institute Inc.), along with cycloheximide (CHX), in starvation medium (DMEM containing 0.1% BSA) for 3 hours, and then stimulated with 100 ng/ml hEGF (PeproTech).

Plasmids

A wild-type AMSH expression vector, p3xFLAG-AMSH, was generated by inserting the human AMSH cDNA into p3xFLAG-CMV-10 (Sigma). Mutant AMSH expression vectors were generated by PCR-based procedures (Kobayashi *et al.*, 2005). An expression plasmid for a catalytically inactive AMSH, p3xFLAG-AMSH^{E280A}, was generated using the QuickChange™ site-directed mutagenesis kit (Stratagene) according to the manufacturer's instructions. For the EGFP-tagged AMSH expression, pEGFP-AMSH was generated by inserting the PCR-amplified cDNA into pEGFP-C3 (Clontech). For the expression of GST-fused recombinant AMSH and CHMP3, pGEX-6P-3-AMSH and pGEX-6P-3-CHMP3 were generated using pGEX-6P-3 (GE Healthcare). pMyc-CHMP3 is an expression vector for the Myc-tagged wild-type CHMP3, constructed by inserting the human CHMP3 cDNA into pcDNA-Myc (Invitrogen). Myc-tagged CHMP3 mutants were generated by a PCR-based method. pDsRed-CHMP3 was constructed by inserting the CHMP3 cDNA into pDsRed-Monomer-N1 (Clontech). pcDNA3.1-V5-CHMP2A and pcDNA3.1-V5-CHMP2B are expression vectors for wild-type CHMP2A and 2B, constructed using pcDNA3.1/V5-HisA (Invitrogen). p3xFLAG-VPS4 and p3xFLAG-VPS4^{E228Q} were generated by inserting the PCR-amplified cDNAs into p3xFLAG-CMV-10. pcDNA3.1-V5-EGFR was generated using pcDNA3.1-V5 (Invitrogen). pcDNA3.1-Myc-Ubiquitin is an expression vector for wild-type Ubiquitin, constructed by inserting the Ubiquitin cDNA into pcDNA3.1/Myc-HisA (Invitrogen). HA-c-Cbl is an HA-tagged E3 ubiquitin ligase that targets EGFR, and was a generous gift from Dr Yosef Yarden (Weizmann Institute of Science). The DNA sequences were verified using a DNA sequencer (ABI3100, Applied Bioscience) and the BigDye Terminator kit (Applied Bioscience).

Immunoprecipitation and immunoblots

Immunoprecipitation and immunoblotting were carried out as

described previously. In brief, cells were lysed in the NP-40 Lysis buffer (1% Nonidet P-40, 40 mM Tris-HCl [pH 7.5], 150 mM NaCl, 2 mM EDTA, 1 mM phenylmethylsulfonyl fluoride, and 20 μg/ml aprotinin). The cell lysates were pre-cleared of cellular debris by centrifugation (10,000×g) for 30 min at 4°C, and then subjected to immunoprecipitation with antibodies immobilized on Protein A-Sepharose beads (GE Healthcare) at 4°C, overnight. For this assay, the monoclonal antibodies (mAbs) anti-Myc (Santa Cruz), anti-FLAG-M2 (Sigma), anti-V5 (Invitrogen), anti-LAMP1 (Santa Cruz), and anti-AMSH (Tanaka *et al.*, 1999), and polyclonal anti-α-tubulin (Sigma) were used. Anti-CHMP3 antisera were prepared by immunizing rabbits with recombinant full-length human CHMP3 protein. The immunoprecipitates were separated by SDS-PAGE and transferred onto PVDF membranes (Millipore). After blocking with 5% nonfat milk in Tris-buffered saline (TBS) containing 0.1% Tween 20, the membranes were probed with the indicated primary antibodies. After three washes, the membranes were probed with HRP-conjugated secondary antibodies (Cell Signaling Technology). Signals were visualized with a Super signal pico detection kit (Pierce), and digital images were collected with a Lumi-Imager F1 (Roche).

Preparation of cytosol and membrane fractions

Cells were washed with PBS and lysed in homogenization buffer (10 mM HEPES, 3 mM imidazole, 250 mM sucrose) by repeated passage through a 22G needle at 4°C. A postnuclear fraction (PNF) supernatant was obtained by centrifugation for 10 min at 3000×g. The PNF was subjected to ultracentrifugation for 30 min at 100,000×g, and the cytosolic and membrane fractions were separated.

Preparation of bacterially expressed recombinant proteins and a GST pull-down assay

GST-CHMP3 (2 μg), purified from *E. coli* BL21, was incubated with cell lysates prepared from 293T cells transfected with various AMSH-expression vectors and further mixed with 10 μl of Glutathione-Sepharose beads (GE Healthcare) for one hour, at 4°C. The beads were extensively washed with the NP-40 Lysis buffer, and proteins associated with the beads were subjected to immunoblotting with anti-GST antisera (MBL) or anti-FLAG-M2 mAb. Likewise, GST-AMSH recombinant protein was used to detect the association with various CHMP3 constructs expressed by the transfected 293T cells. For controls, 2% of the transfected cell lysate was used to monitor the protein.

In vitro deubiquitination assay

K48-linked or K63-linked polyubiquitin chains (500 ng; Boston Biochem) were incubated with 5 μg of GST-fusion proteins at 37°C for 18 hours in DUB buffer (PBS [pH 7.0], 5 mM $MgCl_2$, 2 mM DTT) (Mizuno *et al.*, 2005). Tris-Tricine Sample Buffer (0.1 M Tris-HCl [pH 6.8], 24% Glycerol, 1% SDS, 2% β-mercaptoethanol, and 2% Coomassie G-250) was added, and the reaction mixture was heated to 95°C for 5 minutes and resolved on 16.5% Ready Gels J Peptide (BioRad). Ubiquitin was detected using an anti-ubiquitin mAb, P4D1 (Santa Cruz).

Depletion of cellular AMSH by shRNA

A human AMSH-specific short hairpin RNA (shRNA), pSIREN-RetroQ-AMSH was generated using pSIREN-RetroQ (BD Biosciences). The target sequences within human AMSH cDNA were nucleotide residues 651–669 (5'-GCAGCAATTGGAACAGGAA-3') and 463–481 (5'-GTAAAGAAATTAAAGGAGA-3'). A control plasmid, pSIREN-RetroQ-pRL-Null, targeted the 413–434 (5'-GCAATAGTTCACGCTGAAAAG-3') sequence of the firefly luciferase gene. For retrovirus-mediated transfer of these constructs, 293T cells in 10-cm dishes were transfected with 15 μg of pSIREN-RetroQ-AMSH along with 10 μg of pMD.G (a gift from Dr. I. M. Verma) and 5 μg of gagpol-IRES-bsr (a gift from Dr. T. Kitamura), by the calcium phosphate precipitation method. At 12 hours post-transfection, the cell culture medium was replaced. At 48 hours post-transfection, the supernatants were collected, filtered through a 0.45-μm syringe filter, and spun at 6,000×*g* for 20 hours at 4°C. The virus obtained from the pellet was used for further transduction experiments.

Immunofluorescence microscopy and immunolabeling

HeLa cells were grown in 35-mm glass-bottomed dishes (Matsunami) at a density of 4×10^4 cells/dish and transfected with pDsRed1-CHMP3 or pEGFP-AMSH. After 48 hours, the cells were washed twice with phosphate-buffered saline (PBS), fixed with 4% paraformaldehyde (PFA) for 15 min, washed in wash buffer (0.1% TritonX-100/PBS), and then blocked in the same buffer containing 10% FCS. For immunostaining, the fixed samples were incubated in wash buffer containing 5% FCS at 4°C overnight with the indicated primary antibodies: anti-EEA1, anti-LAMP2 antisera (Santa Cruz), and anti-LAMP1 (Santa Cruz), anti-LBPA (a gift from Dr. T. Kobayashi) (Kobayashi *et al.*, 1998), and FK2 (Affiniti Research Products) mAbs. The anti-AMSH antiserum was described previously (Tanaka *et al.*, 1999). After three washes, the samples were further incubated with the secondary antibodies (anti-rabbit, -mouse, and -goat IgG antibodies conjugated with Alexa488, Alexa594, and Alexa633, respectively, Molecular Probes) at room temperature for one hour. The confocal microscopic images were examined using the 510 META microscope with a 60/1.30–0.60 oil-immersion objective (Carl Zeiss).

Immuno-electron microscopy

For immuno-electron microscopy, the pre-embedding silver-enhanced immunogold method was performed as previously described (Yoshimori *et al.*, 2000). HeLa cells were cultured on plastic coverslips (LF; Sumitomo Bakelite).

Results

AMSH associates with the ESCRT-III protein CHMP3

To explore the function of AMSH on endosomes, we used a co-immunoprecipitation-based strategy to identify AMSH-binding proteins. 3×FLAG-tagged AMSH was expressed in 293T cells, and the anti-FLAG mAb-directed immunoprecipitates were analyzed using MALDI-TOF MASS spectrometry. Among the immunoprecipitates was a 33-kDa band corresponding to human CHMP3, an ESCRT-III subunit (Supplementary Fig. S1). To verify the association between AMSH and CHMP3, we performed co-immunoprecipitation assays of the FLAG-tagged AMSH and myc-tagged CHMP3. The association of these two molecules was clearly observed in the immunoblotted immunoprecipitates only when both proteins were transiently expressed in the 293T cells (Fig. 1A). To confirm this association in native cells, we performed a co-immunoprecipitation assay using HeLa cells. Anti-AMSH mAb-directed immunoprecipitates included CHMP3, although we could not detect AMSH in immunoprecipitates brought down with anti-CHMP3 antisera (Fig. 1B). Next, to clarify the CHMP3-association site within AMSH, we performed GST pull-down assays using the following AMSH mutants: AMSH^{dN1}, AMSH^{dN2}, AMSH^{dN3}, AMSH^{dCC}, AMSH^{dSBM}, and AMSH^{dBS3} (see Fig. 1C). GST-CHMP3 showed direct binding to wild-type AMSH expressed in 293T cells as well as to AMSH^{dCC}, AMSH^{dSBM}, and AMSH^{dBS3}, whereas CHMP3 did not associate with AMSH^{dN1}, AMSH^{dN2}, or AMSH^{dN3} (Fig. 1D). We next examined which region within CHMP3 is required for its association with AMSH using the CHMP3 mutants depicted in Fig. 1E. As shown in Fig. 1F, pull-down experiments revealed that the association of CHMP3 with AMSH requires the carboxy-terminal region of CHMP3, including the third coiled-coil region (CC3). Collectively, these results indicate that AMSH binds CHMP3 *in vivo* through its N-terminal region, and the CC3 region of CHMP3 is required for the association.

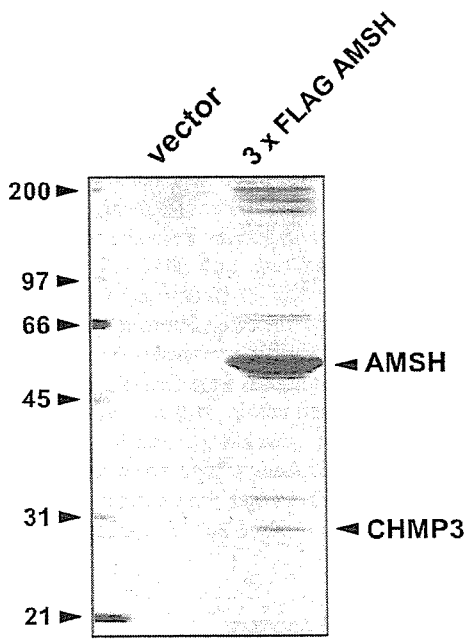

Supplementary Fig. S1. SDS-PAGE analysis of the AMSH interacting proteins. 3×FLAG tagged AMSH (right lane) or a control vector (left lane) was transiently transfected in 293T cells. Lysates were obtained from 100 dishes (14.5 cm diameter). One hundred microgram proteins from each sample were separated by SDS-PAGE. Silver staining was shown. AMSH and CHMP3 (arrowheads) were identified from a mass spectrometry. Analyses for other proteins are underway.

AMSH co-localizes with CHMP3 on endosomes

CHMP3's known identity as one of the ESCRT-III subunits (Morita and Sundquist, 2004; Babst, 2005) led us to investigate whether AMSH co-localizes with CHMP3 on maturing endosomes. To clarify the intracellular localization of AMSH, we transfected HeLa cells with a CHMP3 expression vector and analyzed the localization of the exogenous CHMP3 as well as the endogenous AMSH by confocal microscopy. In accordance with previous findings (Itoh *et al.*, 2001; McCullough *et al.*, 2004), we detected AMSH as scattered puncta throughout the cytoplasm with moderate expression in the nucleus (Fig. 2A). In addition to the AMSH co-localization with early endosomes, we found clear evidence that AMSH was located on the MVB and late endosomes, as determined by co-staining with LBPA and LAMP1, respectively. Interestingly, although AMSH and CHMP3 were co-localized at the LBPA-positive and the LAMP1-positive vesicles (Fig. 2A, middle and bottom panels, arrowheads), they showed little co-localization with early endosomes (Fig. 2A, top panels, arrowheads). These results suggest that AMSH and CHMP3 co-localize on maturing endosomes rather than early endosomes, although AMSH without CHMP3 is present on early endosomes.

We also examined the localization of exogenous, GFP-tagged AMSH and its mutants, to learn what role CHMP3 plays in the localization of AMSH. As previously reported, GFP-tagged AMSH was seen co-localized with early endosomes (Fig. 2B, arrowheads), but it was associated with late endosomes to a lesser extent (Fig. 2B, arrows). Next, we examined whether an AMSH mutant devoid of the CHMP3-binding capability still localized to endosomes. Unexpectedly, AMSH^{dN3} showed a similar localization pattern to wild-type AMSH, in that AMSH^{dN3} was clearly localized to both the early and late endosomes (Fig. 2B, arrowheads and arrows, respectively). In addition, the introduction of AMSH^{dN3} induced a moderate increase in aberrant AMSH/LAMP1/EEA1-positive endosomes (Fig. 2B, bottom panels, asterisks). We therefore concluded that the AMSH-

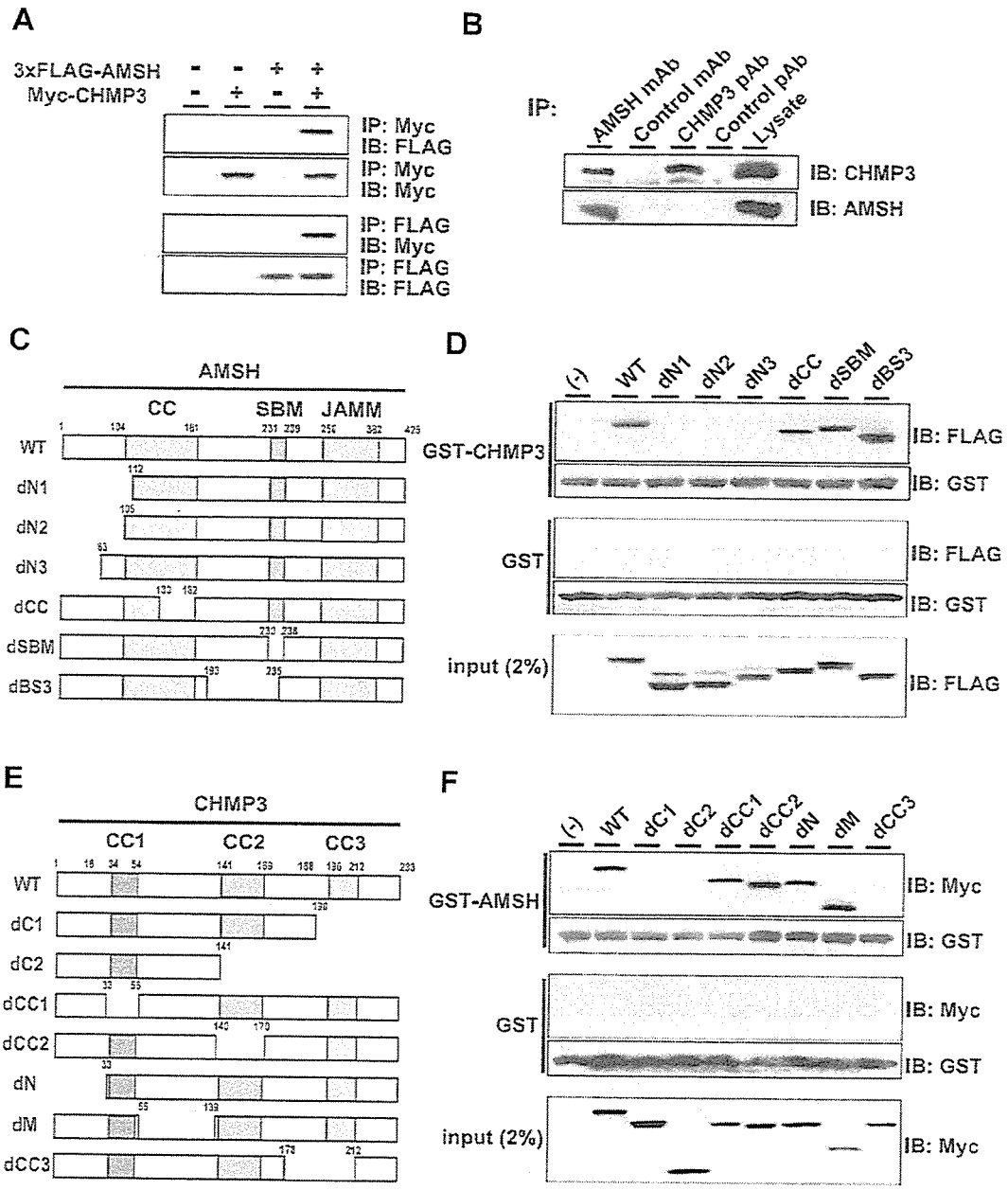

Fig. 1. Identification of CHMP3 as an AMSH-binding protein. (A) AMSH binds CHMP3 in 293T cells. Cells were transfected with pMyc-CHMP3, p3xFLAG-AMSH. After 48 hours, the cell lysates were used for immunoprecipitation (IP) and immunoblotting (IB) with the indicated antibodies. (B) AMSH binds endogenous CHMP3. HeLa cells in culture were subjected to chemical crosslinking by 100 μg/ml DSP. The cell lysates were used for immunoprecipitation by anti-AMSH, control mAbs, anti-CHMP3, and pre-immune antisera, respectively. Immunoblotting was performed with anti-CHMP3 antisera. Approximately 5% of the prepared lysates was used for the anti-CHMP3 IP and for the total cell lysate (Lysate) lanes. (C) Structures of wild-type AMSH and its mutants; (dN1, AMSH^{dN1}; dN2, AMSH^{dN2}; dN3, AMSH^{dN3}; dCC, AMSH^{dCC}; dSBM, AMSH^{dSBM}; dBS3, AMSH^{dBS3}). CC, SBM, and JAMM stand for the coiled-coil region, STAM-binding motif, and JAMM domain, respectively. (D) CHMP3 binds to the N-terminal region of AMSH *in vitro*. (Top) Proteins pulled down by GST-CHMP3 were immunoblotted with the anti-FLAG mAb or anti-GST antisera, as indicated. (Middle) For a control study, proteins pulled down by GST were immunoblotted with the anti-FLAG mAb or anti-GST antisera, as indicated. (Bottom) 2% of the input is shown. (E) Structures of wild-type CHMP3 and its mutants; (dC1, CHMP3^{dC1}; dC2, CHMP3^{dC2}; dCC1, CHMP3^{dCC1}; dCC2, CHMP3^{dCC2}; dN, CHMP3^{dN}; dM, CHMP3^{dM}; dCC3, CHMP3^{dCC3}). (F) AMSH binds to the coiled-coil3 region of CHMP3 *in vitro*. (Top) Proteins pulled down by the GST-CHMP3 were immunoblotted with the anti-Myc or anti-GST antisera. (Middle) For a control study, proteins pulled down by GST were immunoblotted with the anti-Myc or anti-GST antisera, respectively. (Bottom) 2% of the input is shown.

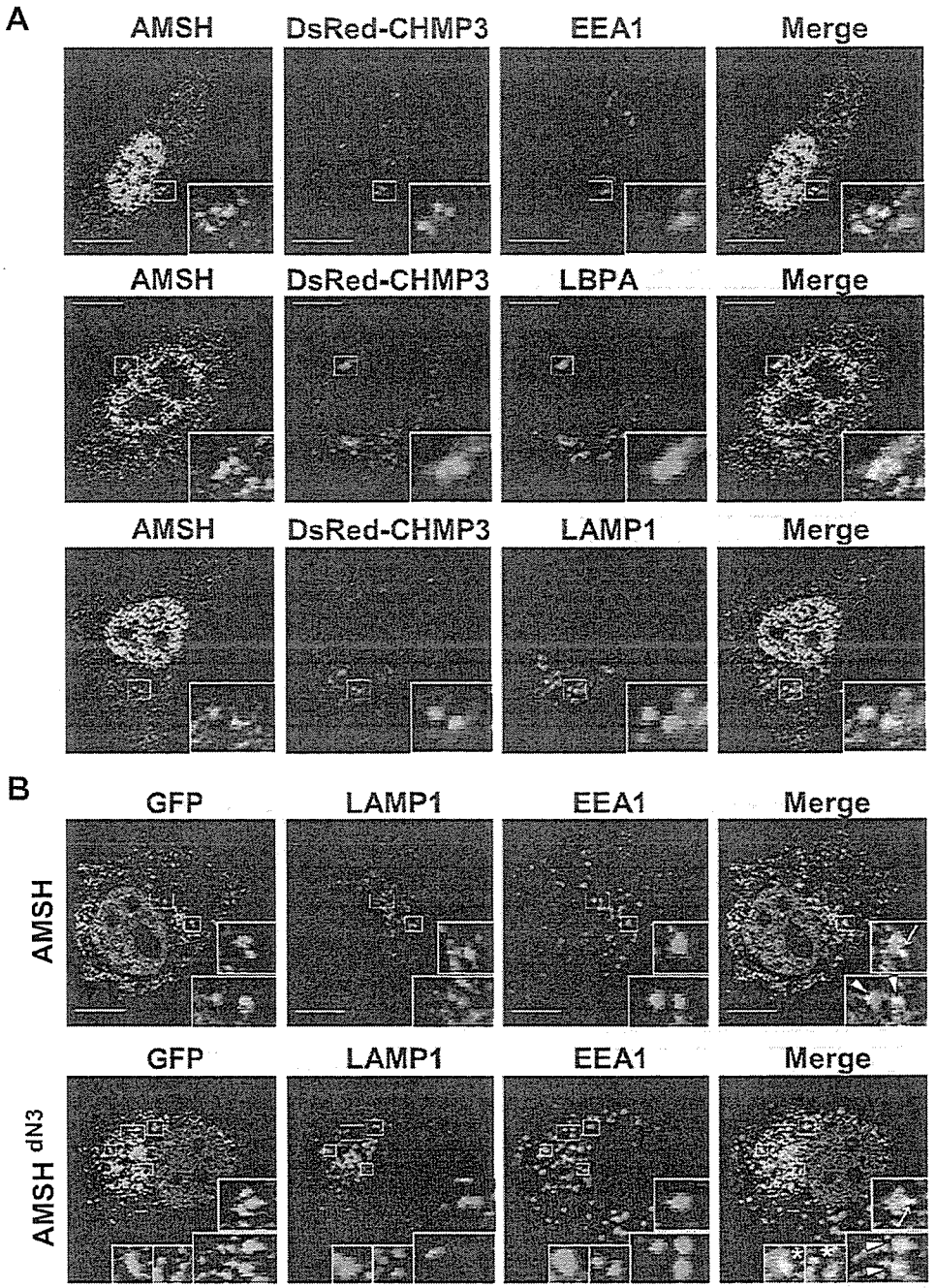

Fig. 2. AMSH co-localizes with CHMP3 on MVB/late endosomes, but the CHMP3-binding region is not required for this localization. (A) Co-localization of AMSH and CHMP3 on MVB/late endosomes. HeLa cells were transfected with pDsRed-Monomer-CHMP3. After 48 hours, cells were double-labeled with the antibodies indicated on the figure. (Top) AMSH (green), DsRed-CHMP3 (red), and EEA1 (blue). (Middle) AMSH (green), DSRed-CHMP3 (red), and LBPA (blue). (Bottom) AMSH (green), DS-redCHMP3 (red), and LAMP1 (blue). Green labeling is from Alexa 488-conjugated secondary antibody; blue is from Alexa 633-conjugated secondary antibody. Insets show magnification of boxed areas. Arrowheads indicate colocalization of AMSH with DsRed-CHMP3 (Top), DsRed-CHMP3 and LBPA (Middle), DsRed-CHMP3 and LAMP1 (Bottom), receptively. (B) Localization of wild-type AMSH and its dN3 mutant. HeLa cells were transfected with pEGFP-AMSH or pEGFP-AMSH^{dN3}. After 48 hours, the cells were double-labeled with the indicated antibodies: LAMP1 (red) and EEA1 (blue). Insets show magnification of boxed areas. Arrowheads indicate colocalization of GFP-AMSH or GFP-AMSH^{dN3} with EEA1. Arrows indicate colocalization of GFP-AMSH or GFP-AMSH^{dN3} with LAMP1. Asterisks indicate colocalization of GFP-AMSH^{dN3} with EEA1 and LAMP1. Fluorescent labeling is as described for (A), except red is from Alexa 594. Bars indicate 10 μm.